

The LIM Domain of Zyxin Is Sufficient for Force-Induced Accumulation of Zyxin During Cell Migration

Arisa Uemura, Thuc-Nghi Nguyen, Amanda N. Steele, and Soichiro Yamada

Department of Biomedical Engineering, University of California, Davis, California

Supplemental Figures:

Figure S1. Traction force is Rho-kinase dependent. (A) Bright-field and GFP images of a zyxin-GFP expressing cell before (–) and after Y27632 (+) addition. The arrowheads point to a pillar that straightens with the Y27632 addition. (B) Plot of the total accumulated zyxin-GFP intensity at adhesion sites (solid black line), total cellular intensity of zyxin-GFP (dashed black line), and total traction force (blue line, secondary axis) before and after (*) the addition of Y27632. Inset, an overlay of GFP and bright-field of an example pillar shown in A. (C) Bright-field and GFP images of a zyxin-GFP expressing cell before (–) and after blebbistatin (+) addition. Time in minutes. Scale bar, 10 μm .

Figure S2. Zyxin accumulation at trailing edge of migrating cell. GFP-tagged zyxin expressing cells are seeded onto a force sensing pillar array. Unlike the leading edge of migrating cells, the zyxin-GFP intensity remains at the cytoplasmic level at the trailing edge. Arrow heads indicate the reference position of the pillar.

Figure S3. Zyxin-deficient cells exert similar traction force as wild-type cells. (A) Both zyxin deficient and wild-type cells were able to exert traction force and bend the pillars coated with fibronectin (arrows). (B) Sum of traction forces at each time point for wildtype and zyxin knockdown cells. (C) Maximum traction force at a single pillar at each timepoint for wildtype and zyxin knockdown cells. (D) Histogram of traction force for wildtype (solid, $n_{\text{pillar}} = 857$) and knockdown (open, $n_{\text{pillar}} = 521$) cells. Scale bar, 10 μm .

Figure S4. Localization of truncated zyxin LIM domains at focal adhesions formed on a flat surface. (A) Immuno-fluorescence analysis of individual LIM motifs transfected cells using paxillin antibody. (B) Immuno-fluorescence analysis of LIM12 or 23 transfected cells using paxillin antibody. Scale bar 10 μm .

Figure S5. Microfabricated force sensing pillar substrate. (A) Scanning electron micrograph of deep-etched silicon master. Scale bar, 5 μm . (B) Bright-field image of collapsed pillars. Scale bar, 10 μm . (C) Top and side views of rhodamine labeled fibronectin coated pillar substrate. The pillars were stained with 2 $\mu\text{g}/\text{mL}$ DiO in ethanol.

Figure S6. Phantom force generation. Migrating cells often rearranged the fibronectin coating, which reorganized to form fibronectin bundles beneath the cells. Cells tugged onto the fibronectin bundles connected to distant pillars, thereby bending them without having the actual cell contact (see arrowheads). The GFP intensity analysis excludes these phantom pillar deformations. Scale bar, 10 μm .

Figure S7. Pillar displacement and GFP intensity analysis. (A) Pillar displacements are calculated based on the difference between the centroids of the undeflected and the deflected pillars. Using ImageJ and bright field image of the pillar array, regions of interest (ROIs, cyan circles with the size of pillar diameter) are placed at the pillar tips. The undeflected positions of all pillars are defined by the median coordinates of the

nearby cell-free pillars in each rows and columns. (B) Since GFP puncta at the pillar tips preferentially accumulated in the direction of the force, the ROI positions are shifted in the direction of deflection by half a pillar diameter to enclose the entire GFP puncta (e.g. red square). In the absence of deflection, the ROIs are not shifted (e.g. yellow square). (C) Each ROI is thresholded to measure mean intensity of the GFP puncta (within the threshold, in red) and the surrounding region of the puncta (outside of the threshold). The mean intensity of each puncta was normalized to the intensity of the corresponding surrounding region. An example of force-bearing contacts with GFP puncta is shown in red square (normalized GFP intensity = 1.788) and force-free contact without GFP puncta (normalized GFP intensity = 1.073) is shown in yellow square.

Supplemental Movies:

Movie S1.

Time-lapse image of the zyxin-GFP expressing cell migrating on the pillar array shown in Figure 1A. Time in minutes and scale bar 5 μm .

Movie S2.

Time-lapse image of the GFP-VASP expressing cell migrating on the pillar array shown in Figure 2A. Time in minutes and scale bar 5 μm .

Movie S3.

Time-lapse image of the zyxin ΔLIM -GFP expressing cell migrating on the pillar array shown in Figure 3C. Time in minutes and scale bar 5 μm .

Movie S4.

Time-lapse image of the zyxin LIM-GFP expressing cell migrating on the pillar array shown in Figure 3E. Time in minutes and scale bar 5 μm .

Movie S5.

Time-lapse image of the zyxin LIM-GFP expressing zyxin knockdown cell migrating on the pillar array shown in Figure 4A. Time in minutes and scale bar 5 μm .

Figure S1

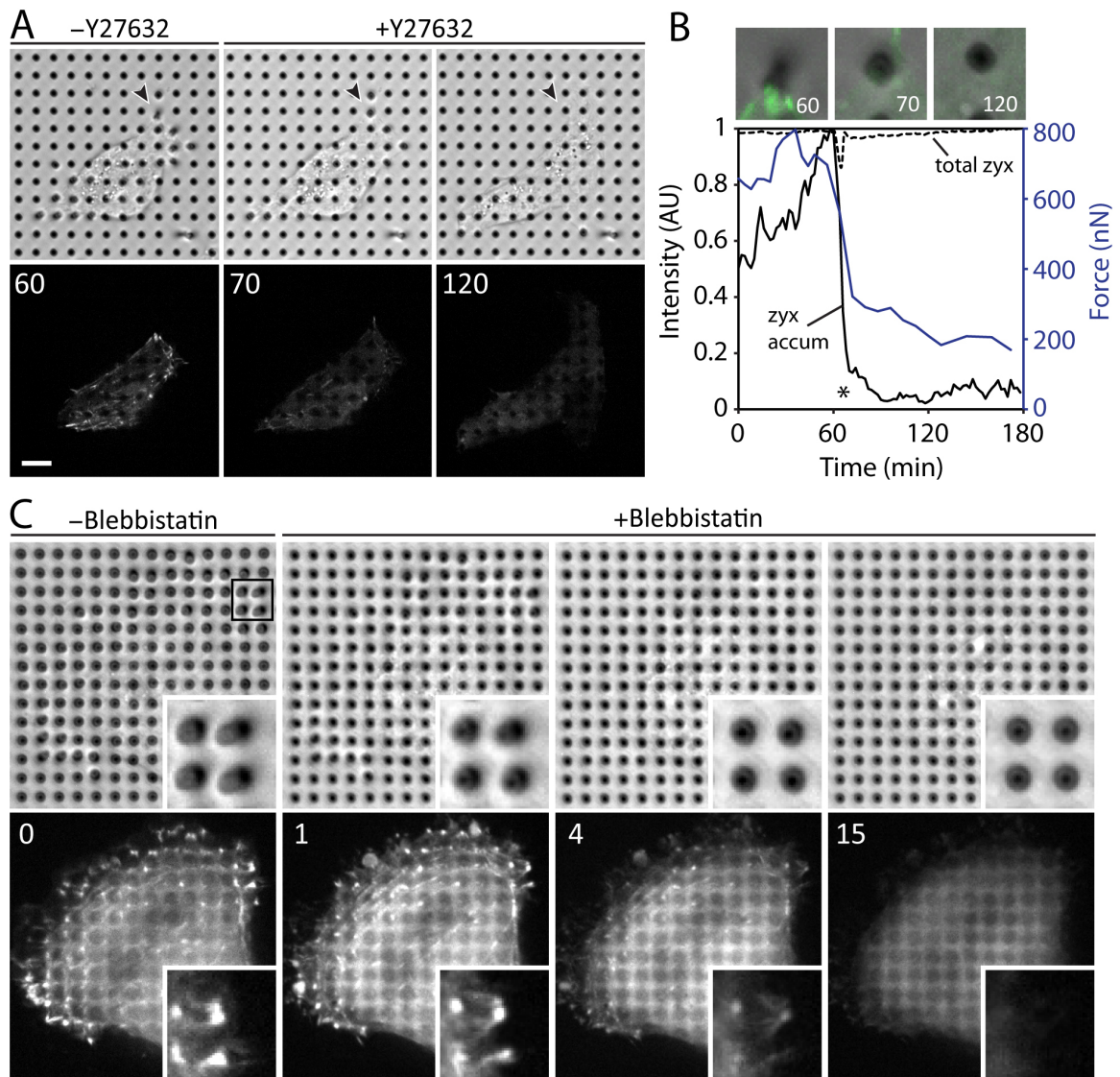


Figure S2

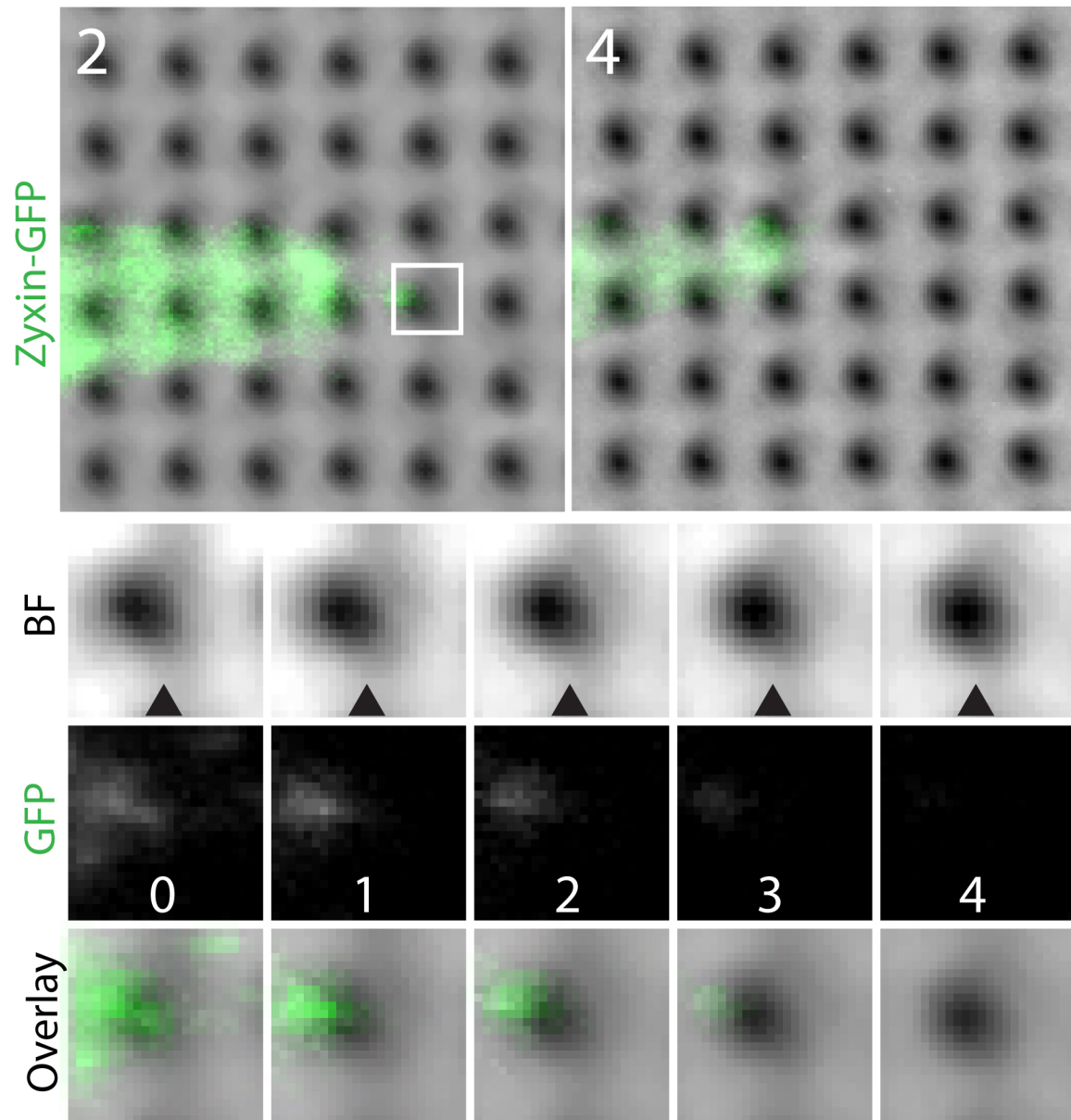


Figure S3

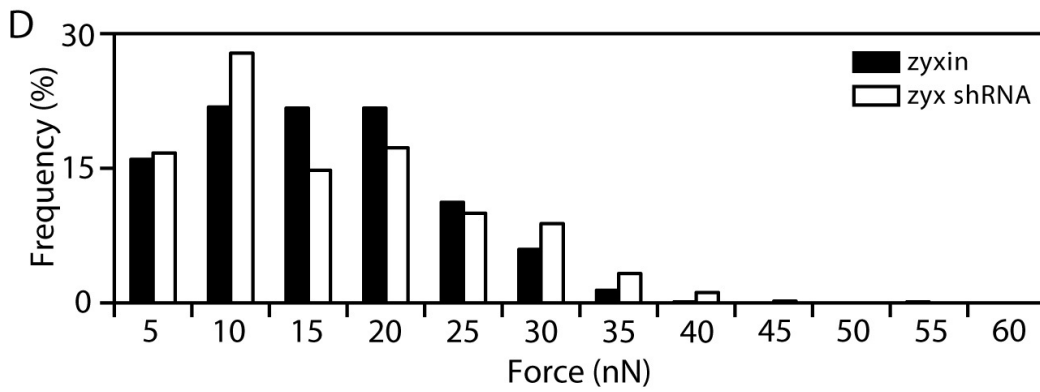
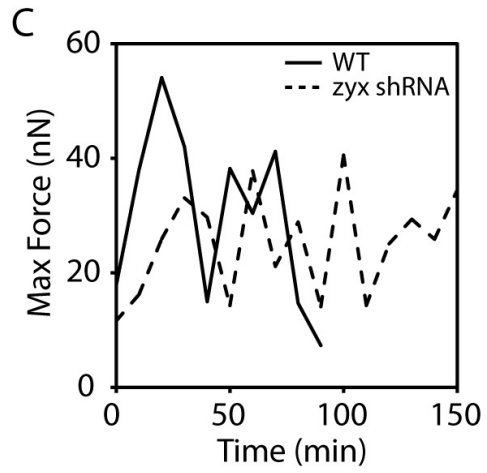
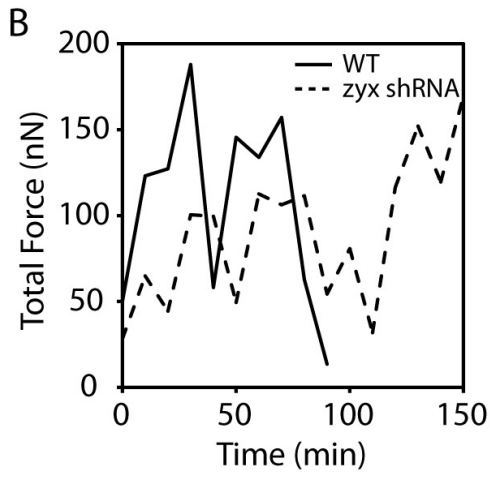
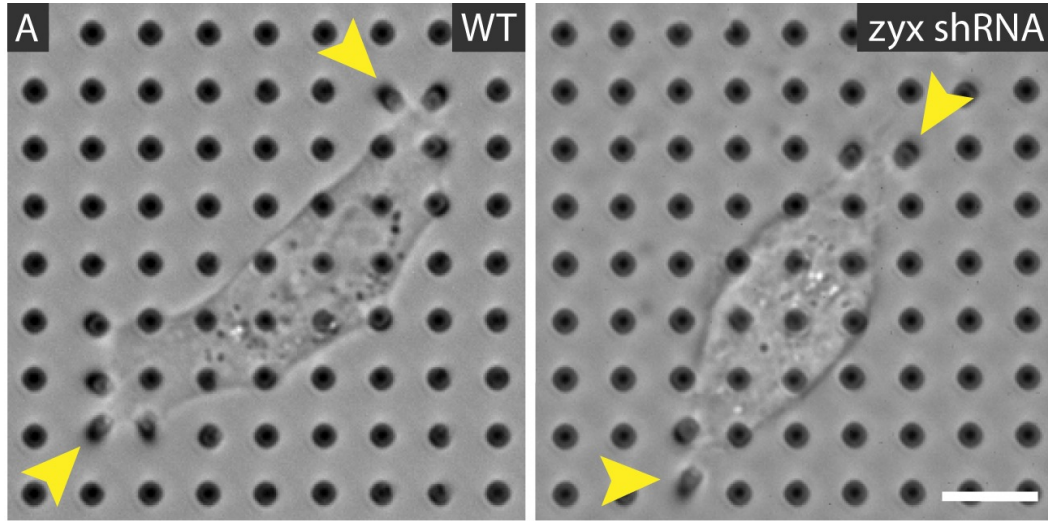


Figure S4

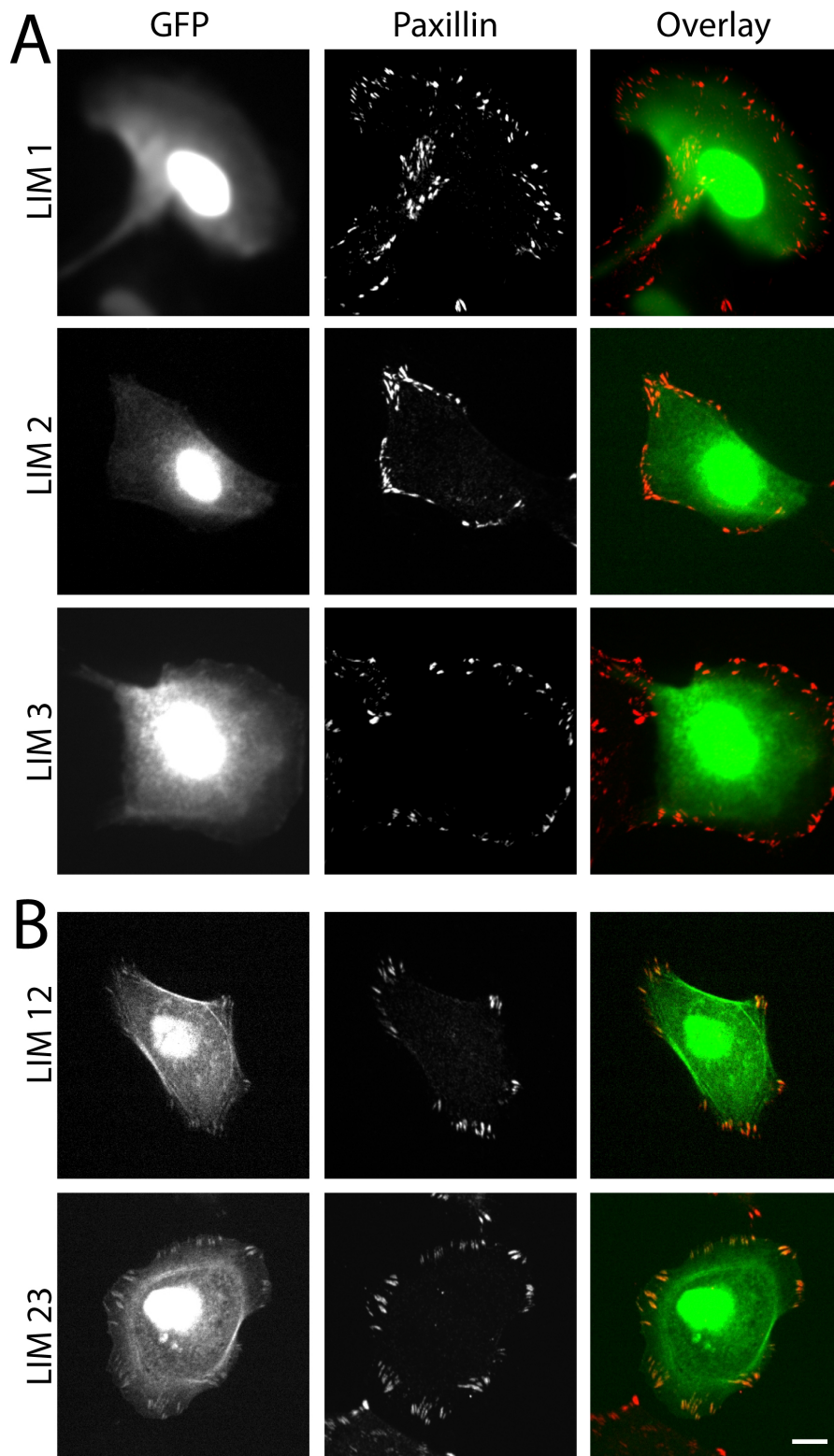


Figure S5

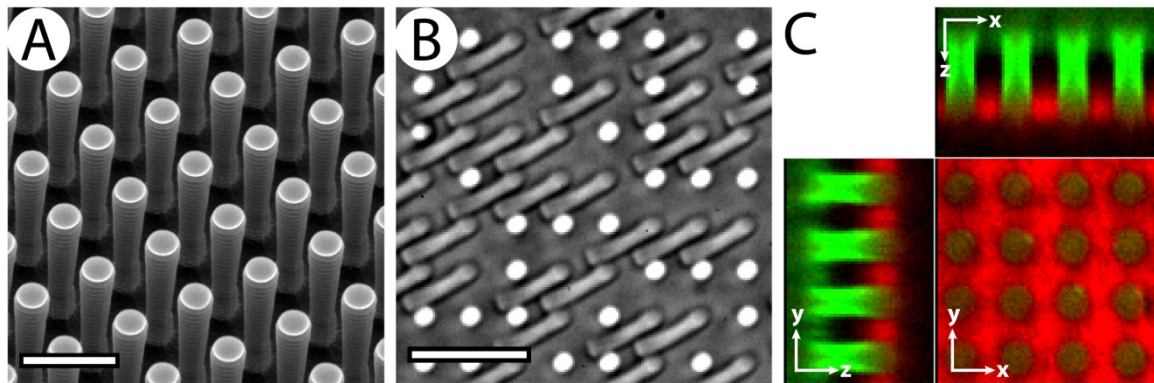


Figure S6

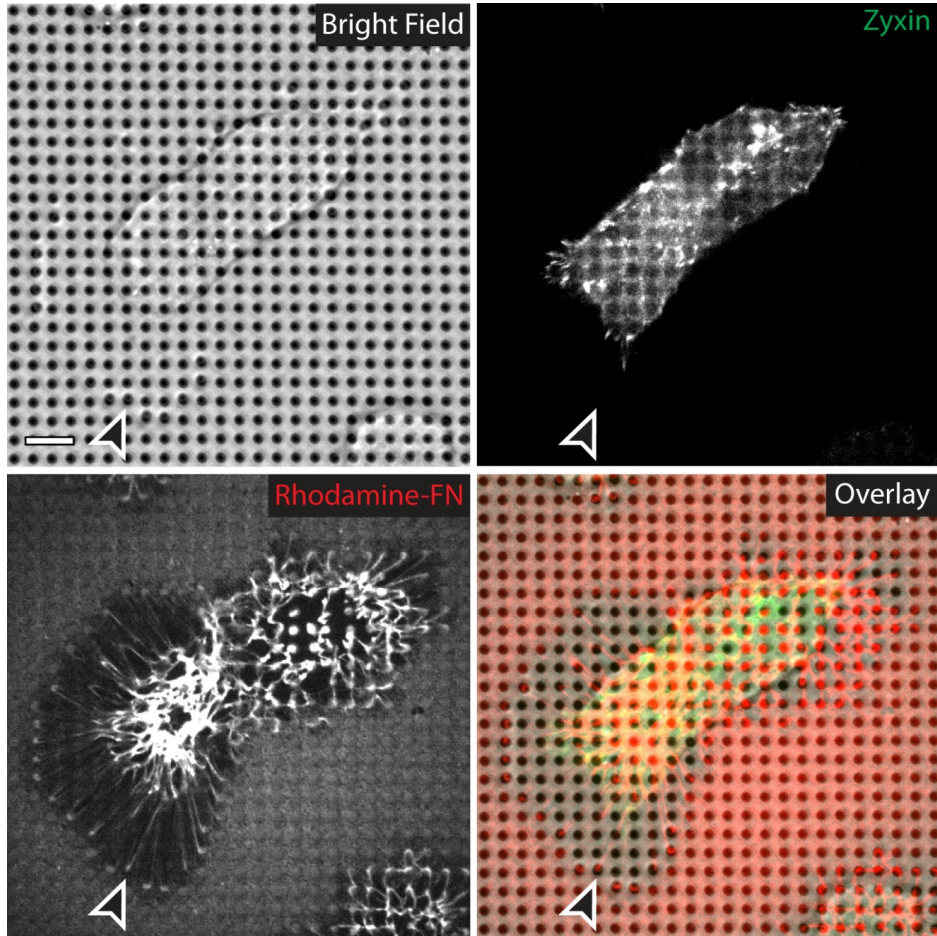


Figure S7

